MultiCraft

International Journal of Engineering, Science and Technology
Vol. 2, No. 1, 2010, pp. 175-191

INTERNATIONAL JOURNAL OF ENGINEERING, SCIENCE AND TECHNOLOGY

www.ijest-ng.com

© 2010 MultiCraft Limited. All rights reserved

A numerical model for the design of a mixed flow cryogenic turbine

Subrata Kr. Ghosh

Department of ME & MME, Indian School of Mines, Dhanbad, Jharkhand, INDIA
E-mail: subratarec@yahoo.co.in

Abstract

Present day cryogenic gas turbines are in more popular as they meet the growing need for low pressure cycles. This calls for improved methods of turbine wheel design. The present study is aimed at the design of the turbine wheel of mixed flow impellers with radial entry and axial discharge. In this paper, a computer code in detail has been developed for designing such turbine wheel. To determine the principal dimensions of the turbine wheel, optimum operating speed has been taken from design charts based on Similarity principles. The algorithm developed, allows any arbitrary combination of fluid properties, inlet conditions and expansion ratio, since the fluid properties are properly taken care of in the relevant equations. The computational process is illustrated with an example. The main dimensions, thermodynamic properties at different states, velocity and angles at entry and exit of the turbine wheel were worked out. The work may help the researchers for further design and development of cryogenic turboexpander depending on their operating parameters.

Keywords: Cryogenic, turboexpander, mixed flow turbine, flow angle, flow velocity

1. Introduction

Compressor, heat exchanger, expansion turbine, and vacuum vessel are the main components to establish any cryogenic liquid plant. To establish the set up, different companies are indigenously available in India for compressor, heat exchanger and vacuum vessel. But the turboexpander is not readily available in market. As the technology is not yet developed indigenously, we are forced to import the whole liquid plant. A simple method sufficient for the design of a high efficiency expansion turbine is outlined by Kun (1987) and Kun *et al*. (1985). A study was initiated in 1979 to survey operating plants and generates the cost factors relating to turbine by Kun & Sentz (1985). They are also sometimes referred to as design parameters, since the shape dictates the type of design to be selected. Corresponding approximately to the optimum efficiency a cryogenic expander may be designed with selected specific speed and specific diameter. Sixsmith et al. (1988) in collaboration with Goddard Space Flight Centre of NASA, developed miniature turbines for Brayton Cycle cryocoolers. Another programme at IIT Kharagpur developed a turboexpander unit by using aerostatic thrust and journal bearings which had a working speed up to 80,000 rpm. The detailed summary of technical features of the cryogenic turboexpander developed in various laboratories has been given in the PhD dissertation of Ghosh (2002). The detailed design parameters for a 90° inward radial flow turbine is shown in the PhD dissertation of Ghosh. Bruce (Bruce, 1998) described the aerodynamic and structural analysis for the complete design of turbo-machinery rotor. The major elements of the turboexpander are briefly discussed in the paper published by Ghosh *et al*. (2005). Baines (2002) has shown that mixed flow turbine concepts can achieve stage loadings that are about 20% greater than those of a conventional radial turbine, without any increase in blade speed and maintaining structural integrity. Descombes (2003) has high-lighted the variability of the local distribution of velocities and pressures within the rotor and gives a real image of energy transformation for nearly ideal zero incidence conditions at the rotor inlet. Abidat (2006) has taken care in the design of the volute essential component of a radial and mixed flow turbines and interest was focused on the influence of the volute inlet flow conditions on its performance. A method of computing blade profiles has been worked out by Hasselgruber (1958), which has been employed by Kun & Sentz (1985) and by Balje (1970, 1981). Effect of some of the turbine operating and design parameters on the flow path and its curvature have been analyzed and presented by Ghosh *et al*. (2009). The computational procedure developed describes the three-dimensional contours of the blades for the turbine wheel.

2. Fluid parameters and layout of components

The fluid specifications have been dictated by the requirements of a small refrigerator producing less than 1 KW of refrigeration. Turbine efficiency of 75% has been assumed following the experience of the workers (Beasley *et al*., 1965; Yang *et al*., 1990; Denton, 1996; Jekat, 1957). The inlet temperature has been specified rather arbitrarily, chosen in such a way that even with ideal (isentropic) expansion; the exit state should not fall in the two-phase region. The basic input parameters for the system are given in Table 1. Figure 1 shows the longitudinal section of a typical cryogenic turboexpander displaying the layout of the components within the system. The major components of the turboexpander are shown in Table 2.

Table 1: Basic input parameters for the cryogenic expansion turbine system

Working fluid	:	Nitrogen	Discharge pressure	:	1.5 bar
Turbine inlet temperature	:	122 K	Throughput	:	67.5 nm3/hr
Turbine inlet pressure	:	6.0 bar	Expected efficiency	:	75%

Table 2: Basic unit of a turboexpander assembly

Turbine wheel	Nozzle	Diffuser	Shaft
Brake compressor	Journal bearings	Thrust bearings	Housing

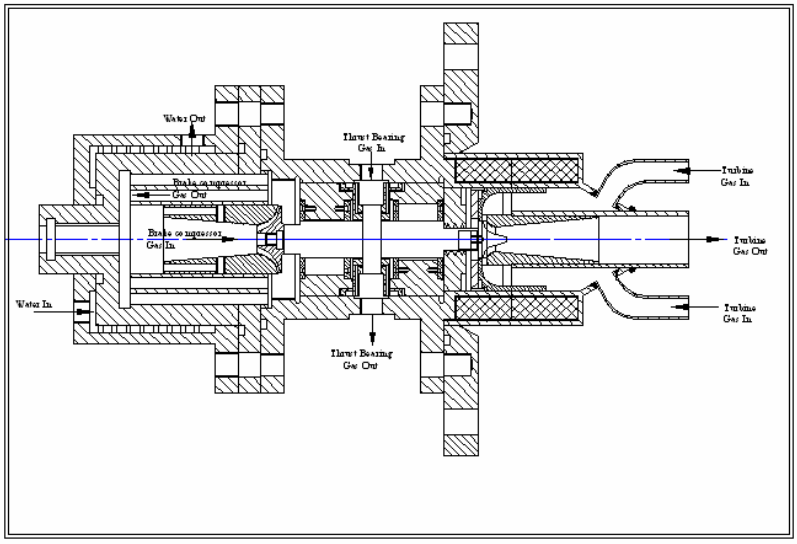

Figure 1: Longitudinal section of the expansion turbine displaying the layout of the components

3. Design of turbine wheel

The design of turbine wheel has been done following the method outlined by Balje (1981) and Kun & Sentz (1985), which are based on the well known "similarity principles". The similarity laws state that for given Reynolds number, Mach number and Specific heat ratio of the working fluid, to achieve optimized geometry for maximum efficiency, two dimensionless parameters: specific speed and specific diameter uniquely determine the major dimensions of the wheel and its inlet and exit velocity triangles. Specific speed (n_s) and specific diameter (d_s) are defined as:

Specific speed
$$n_s = \frac{\omega\sqrt{Q_3}}{\left(\Delta h_{in-3s}\right)^{\frac{3}{4}}} \tag{1}$$

Specific diameter
$$d_s = \frac{D_2 \times \left(\Delta h_{in-3s}\right)^{\frac{1}{4}}}{\sqrt{Q_3}} \tag{2}$$

In the definition of n_s and d_s the volumetric flow rate Q_3 is that at the exit of the turbine wheel. Kun and Sentz (1985), however suggest two empirical factors k_1 and k_2 for evaluating Q_3 and h_{3s}, which define n_s and d_s.

$$Q_3 = k_1 Q_{ex} \text{ and} \tag{3}$$

$$\rho_3 = \rho_{ex} / k_1 \tag{4}$$

$$\Delta h_{in-3s} = k_2 \left(h_{0in} - h_{exs} \right) \tag{5}$$

The factors k_1 and k_2 account for the difference between the states '3' and 'ex' caused by pressure recovery and consequent rise in temperature and density in the diffuser as shown in Figure 2. Following the suggestion of Kun and Sentz (1985), k_2 value is 1.03. The factor k_1 represents the ratio Q_3 / Q_{ex}, which is also equal to ρ_{ex} / ρ_3. The value of Q_{ex} and ρ_{ex} are known at this stage, where as Q_3 and ρ_3 are unknown. By taking a guess value of k_1, the volume flow rate (Q_3) and the density (ρ_3) at the exit condition of the turbine wheel can be calculated from equations (3) and (4) respectively. If the guess value is correct, then Q_3 and ρ_3 should give a turbine exit velocity C_3 that satisfies the velocity triangle as described in equation (13); otherwise the iteration process is repeated with a new guess value of k_1. The value of Q_3 determines turbine exit velocity uniquely. The thermodynamic relations for reversible isentropic flow in the diffuser are,

$$h_{03} = h_{0ex}, \qquad s_3 = s_{ex} \text{ and} \qquad h_3 = h_{03} - \frac{C_3^2}{2}$$

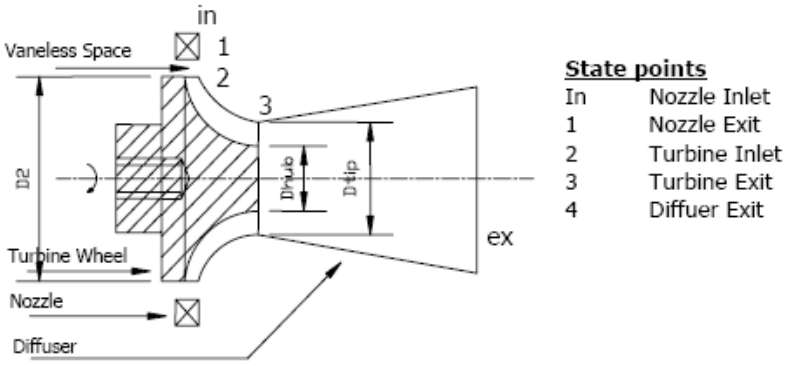

Figure 2: State points of turboexpander

Using the property tables, the value of ρ_3 can be estimated from s_3 and h_3. When the difference between the calculated and initial values of ρ_3 is within the prescribed limit, the iteration is converges. Since the change in entropy in the diffuser is small compared to the total entropy change, assumption of isentropic flow will lead to very little error. The estimation k_1 does not deviate appreciably, if the expansion of fluid from 'in' to 'ex' is non-isentropic. With this assumption, the value of k_1 is estimated to be 1.11, starting with the initial guess value of 1.02. A flow chart for determining the value of k_1 is described in the Figure 9.

For estimating the thermodynamic properties at different states along the flow passage, the software package ALLPROPS 4.2 available from the University of Idaho, Moscow (Lemmon *et al*., 1995) is used. Table 3 represents the thermodynamic states at the inlet of the nozzle and the exit of the diffuser according to input specifications. The exit state has two different columns, one is isentropic expansion and other is with isentropic efficiency of 75%.

Using data from Table 3,

$$\left.\begin{aligned} Q_{ex} &= \frac{\dot{m}_{tr}}{\rho_{ex}} = \frac{23.26 \times 10^{-3}}{5.86} = 3.97 \times 10^{-3} \text{ m}^3/\text{s} \\ \rho_3 &= \frac{\rho_{ex}}{k_1} = \frac{5.86}{1.11} = 5.27 \text{ kg/m}^3 \\ Q_3 &= k_1 Q_{ex} = 4.42 \times 10^{-3} \text{ m}^3/\text{s} \end{aligned}\right\} \tag{6}$$

$$\Delta h_{in-3s} = k_2\left(h_{0,in} - h_{ex,s}\right) = 1.03 \times 38.7 \times 10^3 = 39861 \text{ J/kg}$$

From Balje (1981) the peak efficiency of a radial inflow turbine corresponds to the values of:

$$n_s = 0.54 \text{ and } d_s = 3.4 \tag{7}$$

Substituting these values in equations (1) and (2) respectively, yields

$$\left.\begin{aligned} &\text{Rotational speed} \quad \omega = 22910 \text{ rad/s} = 2{,}18{,}775 \text{ r/min}, \\ &\text{Wheel diameter} \quad D_2 = 16.0 \text{ mm}. \end{aligned}\right\} \tag{8}$$

$$\left.\begin{aligned} &\text{Power produced} \quad \mathrm{P} = \dot{m}\left(\mathrm{h_{0in}} - \mathrm{h_{ex}}\right) = \dot{m}\eta\left(\mathrm{h_{0in}} - \mathrm{h_{exs}}\right) = 0.9 \text{ KW} \\ &\text{Tip speed} \quad U_2 = \omega D_2 / 2 = 183.28 \text{ m/s} \\ &\text{Spouting velocity} \quad \mathrm{C_0} = \sqrt{2\Delta \mathrm{h_{in-exs}}} = 278.20 \text{ m/s and} \\ &\text{Velocity ratio} \quad \frac{U_2}{C_0} = 0.66 \end{aligned}\right\} \tag{9}$$

According to Whitfield and Baines (1990), the velocity ratio U_2/C_0 in a radial inflow turbine generally remains within 0.66 and 0.70. The ratio of exit tip diameter to inlet diameter should be limited to a maximum value of 0.70 (Dixon, 1978; Rohlik, 1968) to avoid excessive shroud curvature. Corresponding to the peak efficiency point (Kun and Sentz, 1985):

$$\xi = \mathrm{D_{tip}} / \mathrm{D_2} = 0.676 \tag{10}$$
$$D_{tip} = 10.8 \text{ mm}$$

Table 3: Thermodynamic states at inlet and exit of prototype turbine

	Inlet	isentropic exit state (*ex,s*)	Actual exit state (*ex*)
Pressure (bar)	6	1.50	1.50
Temperature (K)	122	81.72	89.93
Density (kg/m^3)	17.78	6.55	5.86
Enthalpy (kJ/kg)	119.14	80.44	90.11
Entropy (kJ/kg.K)	5.339	5.339	5.452

Balje (1981) prescribes values for the hub ratio $\lambda = D_{hub} / D_{tip}$ against n_s and d_s for axial flow turbines, but makes no specific recommendation for radial flow machines. In axial flow and large radial flow turbines, a small hub ratio would lead to large blade height, with associated machining difficulties and vibration problems. But in a small radial flow machine, a lower hub ratio can be adopted without any serious difficulty and with the benefit of a larger cross section and lower fluid velocity. According to Rohlik (1968), the exit hub to tip diameter ratio should maintained above a value of 0.4 to avoid excessive hub blade blockage and energy loss. Kun and Sentz (1985) have taken a hub ratio of 0.35 citing mechanical considerations.

$$\lambda = D_{hub} / D_{tip} = .425 \tag{11}$$
$$D_{hub} = 4.6 \text{ mm}$$

There are different approaches for choosing the number of blades, the most common method is based on the concept of 'slip', as applied to centrifugal compressors (Rohlik, 1968; Stewart and Glassman, 1973; Jadeja *et al*., 1985). Denton (1996) has given same guidance on the choice of number of blades by ensuring that the flow is not stagnant on the pressure surface. For small turbines, the hub circumference at exit and diameter of milling cutters available determine the number of blades. In this design the number of blades (Z_{tr}) are chosen to be 10, and the thickness of the blades to be 0.6 mm throughout.
From geometrical considerations:

$$A_3 = \frac{\pi}{4}\left({D_{tip}}^2 - {D_{hub}}^2\right) - \frac{Z_{tr} t_{tr}\left(D_{tip} - D_{hub}\right)}{2\sin\beta_{mean}} \tag{12}$$

$$Q_3 = A_3 C_3 = C_3 \left[\frac{\pi}{4} \left({D_{tip}}^2 - {D_{hub}}^2 \right) - \frac{Z_{tr} t_{tr} \left(D_{tip} - D_{hub} \right)}{2 \sin \beta_{mean}} \right] \tag{13.a}$$

$$Q_3 = C_3 \frac{\pi}{4} \left({D_{tip}}^2 - {D_{hub}}^2 \right) - \frac{Z_{tr} t_{tr} \left(D_{tip} - D_{hub} \right)}{2} \times W_3 \tag{13.b}$$

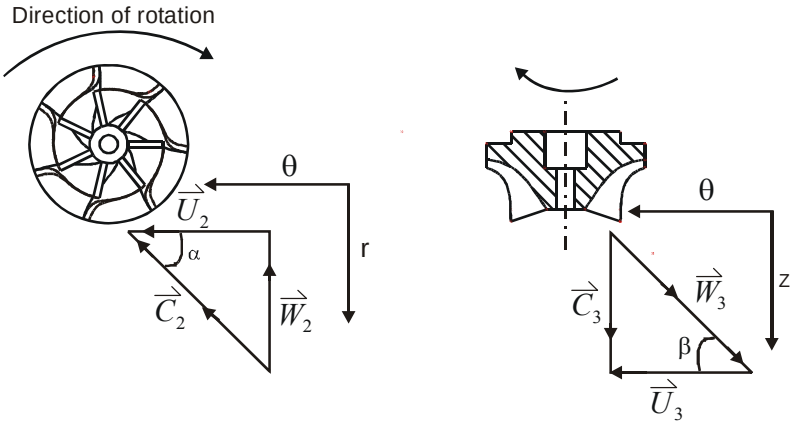

(a) Inlet velocity triangle in the r-θ plane (b) Exit velocity triangle in the θ-z plane.

Figure 3: Inlet and exit velocity triangles of the turbine wheel

From the velocity triangle in Figure 3

$$\tan \beta_{mean} = \frac{C_3}{U_{3,mean}} = \frac{4 C_3}{\omega \left(D_{tip} + D_{hub} \right)} \tag{14}$$

For a given value of Q_3 as given by equation (6), equations (13) and (14) are solved simultaneously for exhaust velocity C_3 and mean relative velocity angle β_{mean}, giving:

$$\left.\begin{aligned} U_{3mean} &= 88.2 \ m/s \\ C_3 &= 90.1 \ m/s \\ \beta_{mean} &= 45.6° \end{aligned}\right\} \tag{15}$$

In summary, the major dimensions for our prototype turbine have been computed as follows:

$$\left.\begin{aligned} &\text{Rotational speed: } N = 22910 \text{ rad/s} = 218{,}775 \text{ rpm} \\ &\text{Wheel diameter: } D_2 = 16.0 \text{ mm} \\ &\text{Eye tip diameter: } D_{tip} = 10.8 \text{ mm} \\ &\text{Eye hub diameter: } D_{hub} = 4.6 \text{ mm} \\ &\text{Number of blades: } Z_{tr} = 10 \\ &\text{Thickness of blades } t_{tr} = 0.6 \text{ mm} \end{aligned}\right\} \tag{16}$$

4. Design of diffuser

For the purpose of design, the diffuser can be seen as an assembly of three separate sections operating in series – a converging section or shroud, a short parallel section and finally the diverging section. The converging portion of the diffuser acts as a casing to the turbine. The straight portion of the diffuser helps in reducing the non-uniformity of flow, and in the diverging section, the pressure recovery takes place.

The geometrical specifications of the diffuser have chosen somewhat arbitrarily. Diameter of diffuser inlet is equal to diameter of the turbine inlet. Diameter of throat of diffuser is dependent on the shroud clearance. The recommended clearance is 2% of the exit

radius, which is approximately 0.2 mm for wheel. The differential contraction between the wheel and the diffuser at low temperature usually acts to enhance this clearance. The profile of the convergent section has been obtained by offsetting the turbine tip profile by 0.2 mm radially. For diameter of diffuser exhaust, Balje (1981) suggested exit velocity of the diffuser should be maintained near about 20 m/s with a half cone angle of 5.5^0. Again by following Ino *et al*. (1992), the best suited diffusing angle $\left(= \tan^{-1} \frac{diameter}{2 * length}\right)$ is 5 to 6 degree which minimizes the loss in pressure recovery and the aspect ratio $\left(= \frac{length}{diameter}\right)$ of 1.4 to 3.3.

With the above recommended suggestions, the dimensions are selected as,

	Diameter of diffuser inlet, D_{inD}	=	16.5 mm.
	Diameter of throat of diffuser, D_{thD}	=	11.0 mm.
	Diameter of diffuser exhaust, D_{exD}	=	19.0 mm.
	Half cone angle	=	5.0^0
giving:	Cross sectional area at throat, A_{thD}	=	95.0 mm^2
	Discharge cross sectional area, A_{thD}	=	283.5 mm^2
	Length of the diverging section L_{dD}	=	45.72 mm

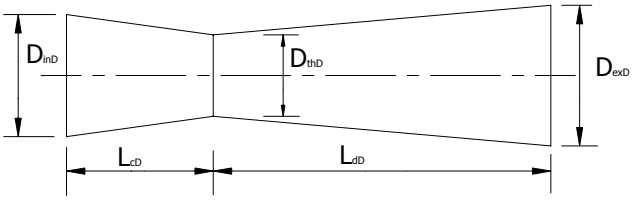

Figure 4: Diffuser nomenclatures

In order to assess the validity of the above dimensions of the diffuser, the Figure 5 is reproduced from Balje (1981). From the figure, in the divergent section, the length to throat radius ratio of 8.31 and exit area to throat area ratio 2.98 give a stable operation of recovery factor of 0.7. This confirms the design of the diffuser.

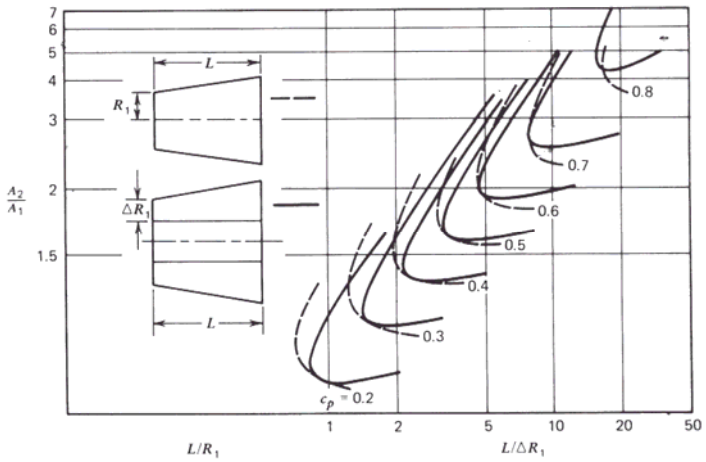

Figure 5: Performance diagram for diffusers (reproduced from Balje (1981))

Thermodynamic state at wheel discharge (state 3)

At the exit of the diffuser,

$$Q_{ex} = 3.97 \times 10^{-3}\ m^3/s \quad \text{and} \qquad A_{ex} = 0.2835 \times 10^{-3}\ m^2$$

Therefore, exit velocity

$$C_{ex} = \frac{Q_{ex}}{A_{ex}} = \frac{3.97 \times 10^{-3}}{0.2835 \times 10^{-3}} = 14.0 \ \text{m/s} \tag{17}$$

This velocity is below 20 m/s as suggested by Balje (1981).

Exit stagnation enthalpy:

$$h_{0ex} = h_{ex} + \frac{{C_{ex}}^2}{2} = 90.11 + \frac{14^2}{2\times10^3} = 90.20 \ \ kJ/kg \tag{18}$$

Exit stagnation pressure:

$$p_{0ex} = p + \frac{1}{2}\rho_{ex}{C^2}_{ex} \approx p \ \text{(as velocity } C_{ex} \text{ is small)} \tag{19}$$

$$= 1.5 + \frac{1}{2}\times 5.86 \times \frac{14^2}{10^5} = 1.505 \ \ bar.$$

Neglecting losses in the diffuser, the stagnation enthalpy at turbine exit,

$$h_{03} = h_{0ex} = 90.20 \ \ kJ/kg\ , \tag{20}$$

From the stagnation enthalpy, h_{03}, and stagnation pressure p_{0ex}, the entropy s_3 is estimated (Lemmon *et al*., 1995) as

$$s_3 = 5.452 \ \ kJ/kg.K$$

and static enthalpy: $$h_3 = h_{03} - \frac{{C_3}^2}{2} = 90.20 - \frac{90.1^2}{2\times1000} = 86.15 \ \ kJ/kg \tag{21}$$

From static enthalpy, $h_3 = 86.15 \ \ kJ/kg$ and $s_3 = 5.452 \ \ kJ/kg.K$, the density ρ_3 calculated (Lemmon *et al*., 1995) as $\rho_3 = 5.26$ kg/m^3.

The choice of $k_1 = 1.11$ is justified by comparing this density value with equations 6. Therefore, the state point 3 is now fully described which can lead to the construction of velocity triangle of the turbine.

Tip circumferential velocity

$$U_{3tip} = \frac{\omega\, D_{tip}}{2} = 22910 \times \frac{10.8}{2\times1000} = 123.7 \ \ \text{m/s} \tag{22}$$

Relative velocity at eye tip

$$W_{3tip} = \sqrt{{U_{3tip}}^2 + {C_3}^2} = \sqrt{123.7^2 + 90.1^2} = 153.0 \ \ \text{m/s} \tag{23}$$

Highest Mach Number

$$\frac{W_{3tip}}{C_{s3}} = \frac{153.0}{184.4} = 0.83 < 1 \tag{24}$$

$$\beta_{3\text{tip}} = tan^{-1}\frac{C_3}{W_{3tip}} = tan^{-1}\frac{90.1}{123.7} = 36.0^{\text{o}} \tag{25}$$

Where C_{s3} is the velocity of sound for the corresponding state point as shown in Table 4.

Similar figures for the eye hub at exit is estimated as

$U_{3hub} = 52.7$ m/s $\quad$ $W_{3\text{hub}} = 104.4$ m/s , and $\quad$ $\beta_{3\text{hub}} = 59.7^{\text{o}}$.

The velocity triangles at the hub, the tip and the mean radius of the eye have been shown in Figure 6. It may be noted that there are two components of velocity, U_2 and W_2 acting on the turbine wheel.

Table 4: Thermodynamic properties at state point 3

	Stagnation value	Static value
Velocity (m/s)	0	90.1
Pressure (bar)	1.505	1.29
Enthalpy (kJ/kg)	90.20	86.15
Entropy (kJ/kg.K)	5.452	5.452
Temperature (K)	90.02	85.96
Density (kg/m^3)	5.89	5.26
Velocity of sound (m/s)	188.87	184.4
Viscosity (Pa.s)	6.13 x 10^{-6}	5.90 x 10^{-6}

Thermodynamic state at wheel inlet (state 2)

For computing the thermodynamic properties at wheel inlet (state 2), the efficiency of the expansion process till state 2 is assumed. Although in high-pressure ratio (~ 10) expansion, the nozzle efficiency η_n is clearly described by Ino *et al*. (1992). Sixsmith (1971) has observed that the nozzle efficiency needs to be between 0.9 and 0.95. Following Kun and Sentz (1985), nozzle efficiency $\eta_n = 0.93$ is assumed. Another important parameter is the ratio of inlet to exit meridional velocities C_{m2}/C_{m3} . Balje (1970) suggests values between 1.0 to 1.25 for this parameter. Following Kun and Sentz (1985), this ratio is assumed to be 1.0, leading to

$$C_{m2} = C_{m3} = C_3 = 90.1 \text{ m/s}. \quad (26)$$

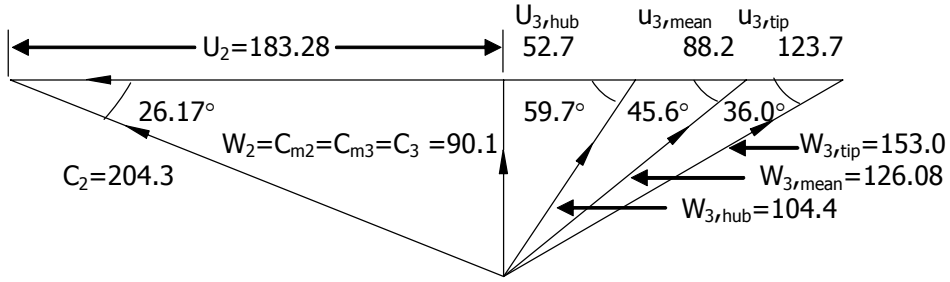

Figure 6: Velocity diagrams for expansion turbine (All velocities are in units of m/s)

The third important assumption relates the gas angle at inlet of the rotor to the corresponding blade angle. Although a negative incidence between 10^o and 20^o has been recommended by authors (Whitfield *et al*., 1990; Rohlik *et al*., 1968), in our design radial blades have been adopted to ensure smooth incidence (Kun *et al*., 1985). Thus

$$W_2 = C_{m2} = 90.1\, m/s \quad (27)$$

Then the absolute velocity at inlet:

$$C_2 = \sqrt{U_2^2 + W_2^2} = \sqrt{183.28^2 + 90.1^2} = 204.3 \text{ m/s} \quad (28)$$

The incidence angle:

$$\alpha_2 = \tan^{-1}\frac{W_2}{U_2} = \tan^{-}\frac{90.1}{183.28} = 26.17^o \quad (29)$$

The efficiency of the nozzle along with the vaneless space is defined as

$$\eta_n = \frac{h_{in} - h_2}{h_{in} - h_{2s}}$$

Since $h_{01} = h_{0in} = h_{in} = 119.14$ kJ/kgK as input parameter, enthalpy at the exit of turbine wheel:

$$h_2 = h_{01} - \frac{{C_2}^2}{2} = 119.14 - \frac{204.3^2}{2 \times 1000} = 98.27 \ \text{kJ/kg} \tag{30}$$

Thus $$h_{2s} = h_{in} - \frac{h_{in} - h_2}{\eta_n} = 96.7 \ \text{kJ/kg} \tag{31}$$

The input parameter for entropy is expressed as:

$$s_{in} = s_1 = s_{2s} = 5.339 \ \text{kJ/kg.K} \tag{32}$$

Using property data (Lemmon *et al*., 1995), the corresponding pressure is calculated from h_{2s} and s_{2s} as:

$$p_{2s} = p_2 = 2.9 \text{ bar}$$

From the values of p_2 and h_2, the other properties at the point 2 is calculated (Lemmon *et al*., 1995) as:

$$T_2 = 99.65 \ K, \quad \rho_2 = 10.42 \ kj/m^3 \ \ and \ s_2 = 5.352 \ kj/kg.K$$

Corresponding to these thermodynamic conditions:

velocity of sound $C_{s2} = 196.85$ m/s,

specific heat $C_p = 1.140$ kJ/kgK and

viscosity $\mu_2 = 6.88 \times 10^{-6}$ pa.s

From continuity equation, the blade height at entrance to the wheel is computed as:

$$b_2 = \frac{\dot{m}_{tr}}{(\pi D_2 - Z_{tr} t_{tr}) \rho_2 C_{m2}} = \frac{23.26 \times 10^{-3} \times 10^6}{(\pi \times 16 - 10 \times 0.6) \times 10.42 \times 90.1} \ \ mm = 0.56 \ \ mm \tag{33}$$

5. Design of the nozzle

An important forcing mechanism leading to fatigue of the wheel is the nozzle excitation frequency. As the wheel blades pass under the jets emanating from the stationary nozzles, there is periodic excitation of the wheel. This periodic excitation is proportional to the speed and the number of nozzle blades (Kun, 1987). The number of nozzle blades is normally dictated by mechanical design consideration, particularly to ensure that nozzle discharge does not excite natural frequency of the impeller (Kun and Sentz, 1985).

The purpose of the nozzle cascade is to assure that the flow should be incident on the wheel at correct angle to avoid incidence loss. Kun and Sentz (1985) selected the nozzle cascade height somewhat smaller than the tip width in order to leave some margin for expansion in the annular space around the wheel and to accommodate axial misalignment. This recommendation, although conforming to common design practice, is too restrictive in case of small turbines. Figure 7 shows the nozzle ring bringing out the major dimensions of the passages and the vanes. The design of the blading system offered no real problem as long as the pressure ratio across the turbine is not more than critical pressure ratio and as long as the temperature drop efficiency demanded does not exceed about 80% (Von Der Nuell, 1952).

Thermodynamic state at the throat and vaneless space

The proposed system uses convergent type of nozzles giving subsonic flow at nozzle exit. Referring to Figure 7 the nozzle throat circle diameter is the outer boundary of the vaneless space while the wheel diameter is the inner circle. If D_t is nozzle throat circle diameter and C_{mt} the meridional component of the nozzle throat velocity, the mass balance equation yields,

$$C_{mt} = \frac{\dot{m}}{\pi D_t b_1 \rho_t} = \frac{23.26 \times 10^{-3} \times 10^6}{\pi \times D_t \times 0.5 \times \rho_t} \tag{34}$$

Where b_1 is the height of the passage, assumed to be 0.5 mm. The velocity at exit of the throat consists of two components, C_{mt} and $C_{\theta t}$. The meridional component is perpendicular to the nozzle throat circle diameter, which determines the mass flow rate whereas the $C_{\theta t}$ other component is tangential to the throat.

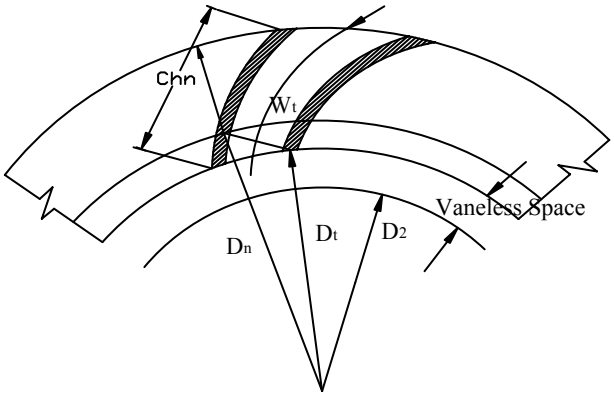

Figure 7: Major dimensions of the nozzle and nozzle vane.

Following Kun and Sentz (1985), $D_t = 1.08 \times D_2 = 17.28 \ \ mm$, leading to

$$C_{mt} = \frac{856.93}{\rho_t} \tag{35}$$

Similar to the presence of two velocity components at the throat circle diameter, there are two velocity components at the entry of the turbine wheel as shown in Figure 3. From conservation of angular momentum in free vortex flow over the vaneless space,

$$C_{\theta t} = \frac{U_2 D_2}{D_t} = \frac{183.28}{1.08} = 169.70 \ m/s \tag{36}$$

Thus, $h_t = h_2 + \frac{{C_2}^2}{2} - \frac{{C_t}^2}{2}$

Since C_t consists of two velocity components perpendicular to each other,

$$h_t = h_2 + \frac{{C_2}^2}{2} - \frac{{C_{mt}}^2}{2} - \frac{{C_{\theta t}}^2}{2} = 119.14 \times 10^3 - \frac{169.70^2}{2} - \frac{{C_{mt}}^2}{2} \ J/kg \ = 104.74 \times 10^3 - \frac{367.16 \times 10^3}{\rho_t^2} \tag{37}$$

The relation between h_t and ρ_t given by equation (37) and the entropy conservation relation given below (Lemmon *et al*., 1995) uniquely determines enthalpy and density at that throat. Assuming isentropic expansion in the vaneless space,

$s_t = s_1 = s_2 = 5.352 \ kJ/kgK$

Solving the above equations,

$h_t = 101.93 \ KJ/kg$ and $\rho_t = 11.45 \ kg/m^3$

Using Ref. (Lemmon *et al*., 1995), the other properties at that throat are found to be

$p_t = 3.30 \ bar$; $T_t = 103.5 \ K$; and $C_{st} = 200.58$ m/s

And the velocities are obtained from equations (35) and (36) as

$C_t = 185.47 \ m/s$; $C_{mt} = 74.84 \ m/s$; and $C_{\theta t} = 169.7 \ m/s$, and

Mach number: $M_t = \frac{C_t}{C_{st}} = 0.92$

This leads to subsonic operation with no loss energy on account of aerodynamic shocks.

Sizing of the nozzle vanes

To compute the dimensions of the throat, Kun & Sentz (1985) used the conservation of momentum & continuity of flow to get the correct throat angle for finite trailing edge thickness. Aerodynamically, it is desirable to make the trailing edge as thin as mechanical design consideration will allow.

Using the Continuity Equation and the density at the throat, the throat width w_t and the throat angle α_t are calculated as follows.

For $\dot{m}_{tr} = \dot{m} = 23.26 \times 10^{-3}$ kg/s and $b_1 = b_t$

$$W_t = \frac{\dot{m}_{tr}}{Z_n b_t \rho_t C_t} = \frac{23.26 \times 10^{-3} \times 10^6}{15 \times 0.5 \times 11.45 \times 185.47} = 1.46\ mm \tag{38}$$

$$\alpha_t = \tan^{-1}\left(\frac{C_{mt}}{C_{\theta t}}\right) = 23.8^o \tag{39}$$

It may be noted that throat inlet angle is different from the turbine blade inlet angle and the discrepancy is due to the drifting of fluid in the vaneless space.

The initial guess value of D_t is checked from the conservation of angular momentum over the vaneless space,

$$D_t = \frac{U_2 D_2}{C_{\theta t}} = 17.28 \text{ mm} \tag{40}$$

which matches to the initial value of 17.28 mm.

The blade pitch length, p_n is estimated as,

$$p_n = \pi D_t / Z_n = 3.62\ mm\ .$$

α_t is the angle between the perpendicular to the throat width w_t and the tangent to the throat circle diameter. From Figure 7, the diameter of the cascade discharge (the inner diameter of the nozzle ring) is calculated as,

$$D_n = \sqrt{{D_t}^2 + {w_t}^2 - 2 w_t D_t Cos\alpha_t} = 26.82 \text{ mm} \tag{41}$$

where α_t is angle between D_t and w_t.

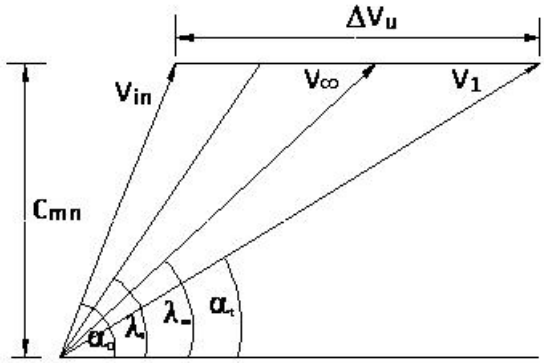

Figure 8: Cascade notation

In cascade theory, blade loading and cascade solidity are defined as:

$$\delta u = \frac{\Delta V_u}{C_{mn}} = \cot\alpha_t - \cot\alpha_0 \qquad \sigma_n = \frac{Ch_n}{S}$$

From cascade notation, $\cot\alpha_t = \cot\lambda_\infty - \frac{\delta u}{2}$ and $\cot\alpha_0 = \cot\lambda_\infty + \frac{\delta u}{2}$

The separation limit, in an approximate way, is expressed by a minimum required solidity. Its value is found from the aerodynamic load coefficient ψ_z defined as the ratio of actual tangential force to ideal tangential force, also known as Zweifel number. The optimum value for the aerodynamic load coefficient is about 0.9. Thus the chord length of nozzle can be found from the equation of solidity and expressed as

$$Ch_n = \frac{2s(\cot\alpha_t - \cot\alpha_0)\sin^2\alpha_t}{\psi_z \sin\lambda_s} = \frac{2\,\delta u \times S}{\psi_z\left[1+\left(\cot\lambda_\infty + \frac{\delta u}{2}\right)^2\right]\sin\lambda_s} \tag{42}$$

Where

S = tangential vane spacing = $\pi D_n / Z_n$ = 4.95 mm.

λ_∞ = cascade angle or mean vector angle = $\cot^{-1}\left(\frac{\cot\alpha_t + \cot\alpha_0}{2}\right)$

λ_s = stagger angle = $\lambda_\infty + \alpha_m$

Following Balje (1981), α_0 is taken as 78° and also gives α_m as a function of $\Delta\lambda = (\alpha_0 - \alpha_t)$ for various values of λ_∞, yields α_m = -4°, leading to: $\delta_u = 2.75$, $\lambda_\infty = 34.2^\circ$, $\lambda_s = 28.2^\circ$ and $Ch_n = 6.58$ mm.

6. Conclusions

A numerical model of the cryogenic turbine wheel has been developed covering hub and tip to study the design and operating parameters on the size of the blade. In addition, the flow chart will play a significant role to find state properties and dimension of cryogenic turboexpander. By using this method the designer is able to get a better feel for the turbine wheel during the design process, he spends less time on mundane data preparation, and he has more freedom to make full use of this creativity to design a better machine. Based on this design, development and experimental work is needed to get the better design and characterize the operation of the devices at higher speeds, including stability, load capacity and heat dissipation. The paper presents an updated literature review on almost all aspects of design of cryogenic turbine, and may serve as a ready reference for future work.

Nomenclature

b	blade height (mm)
C	absolute velocity (m/s)
C_n	chord length of nozzle (mm)
d_s	specific diameter
D	diameter (mm)
h	enthalpy (J / kg)
M	mach number
$\dot{m}$	mass flow rate (Kg/s)
n_s	specific speed
N	rotational speed (rev/ min)
p	pressure (bar)
P	power produced (Kw)
Q	volumetric flow rate (m3 / s)
T	temperature (K)
t	thickness of blades (mm)
U	circumferential velocity (m/s)
W	relative velocity (m/s)
w	width of flow passage (mm)
z	number of blades

Greek symbols

ω	rotational speed (rad/s)
λ	ratio of hub diameter to tip diameter
ε	ratio of tip diameter to turbine wheel diameter
η	isentropic efficiency (dimensionless)
β	relative velocity angle
ρ	density of gas (m3/kg)

Subscripts

0	stagnation condition
1	inlet to nozzle
2	inlet to turbine wheel
3	inlet to the diffuser (exit to wheel)
ex	discharge from diffuser
hub	hub of turbine wheel
tip	tip of turbine wheel
m	meridional component
s	isentropic condition
tr	turbine wheel
n	nozzle
t	throat

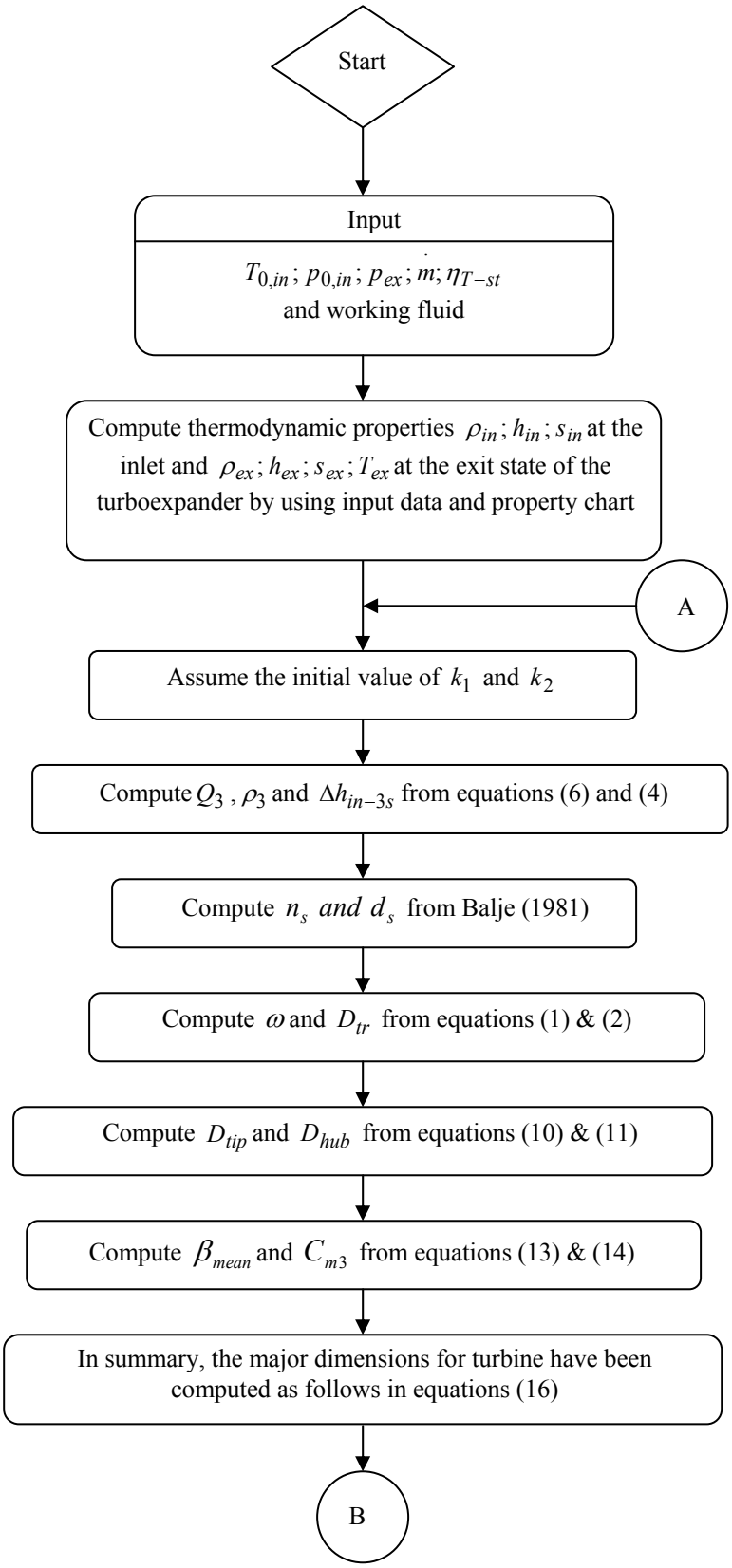
Start
Input
$T_{0,in}$; $p_{0,in}$; p_{ex}; $\dot{m}$; η_{T-st}
and working fluid
Compute thermodynamic properties ρ_{in}; h_{in}; s_{in} at the inlet and ρ_{ex}; h_{ex}; s_{ex}; T_{ex} at the exit state of the turboexpander by using input data and property chart
A
Assume the initial value of k_1 and k_2
Compute Q_3, ρ_3 and Δh_{in-3s} from equations (6) and (4)
Compute n_s and d_s from Balje (1981)
Compute ω and D_{tr} from equations (1) & (2)
Compute D_{tip} and D_{hub} from equations (10) & (11)
Compute β_{mean} and C_{m3} from equations (13) & (14)
In summary, the major dimensions for turbine have been computed as follows in equations (16)
B

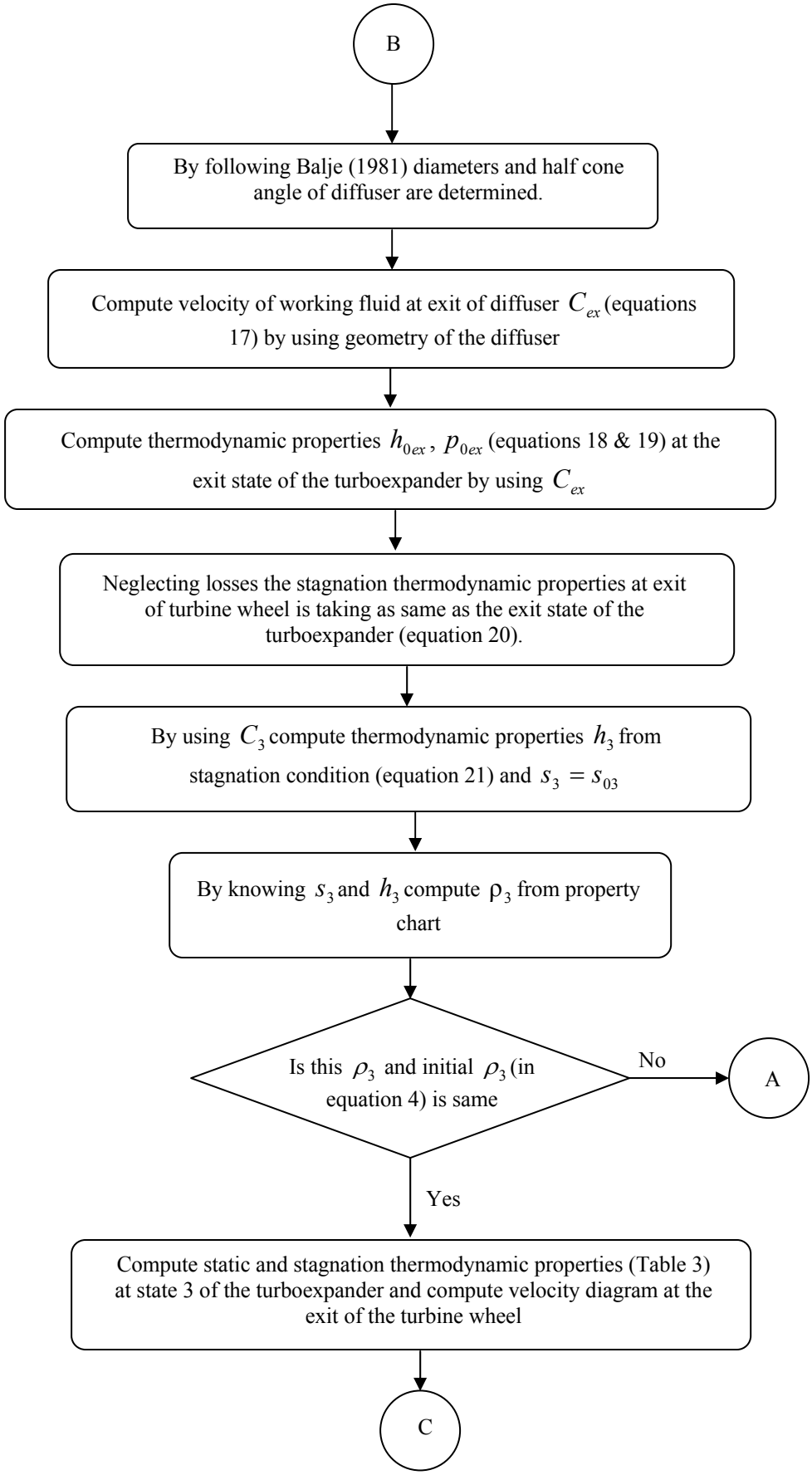
B
By following Balje (1981) diameters and half cone angle of diffuser are determined.
Compute velocity of working fluid at exit of diffuser C_{ex} (equations 17) by using geometry of the diffuser
Compute thermodynamic properties h_{0ex}, p_{0ex} (equations 18 & 19) at the exit state of the turboexpander by using C_{ex}
Neglecting losses the stagnation thermodynamic properties at exit of turbine wheel is taking as same as the exit state of the turboexpander (equation 20).
By using C_3 compute thermodynamic properties h_3 from stagnation condition (equation 21) and $s_3 = s_{03}$
By knowing s_3 and h_3 compute ρ_3 from property chart
Is this ρ_3 and initial ρ_3 (in equation 4) is same
No
A
Yes
Compute static and stagnation thermodynamic properties (Table 3) at state 3 of the turboexpander and compute velocity diagram at the exit of the turbine wheel
C

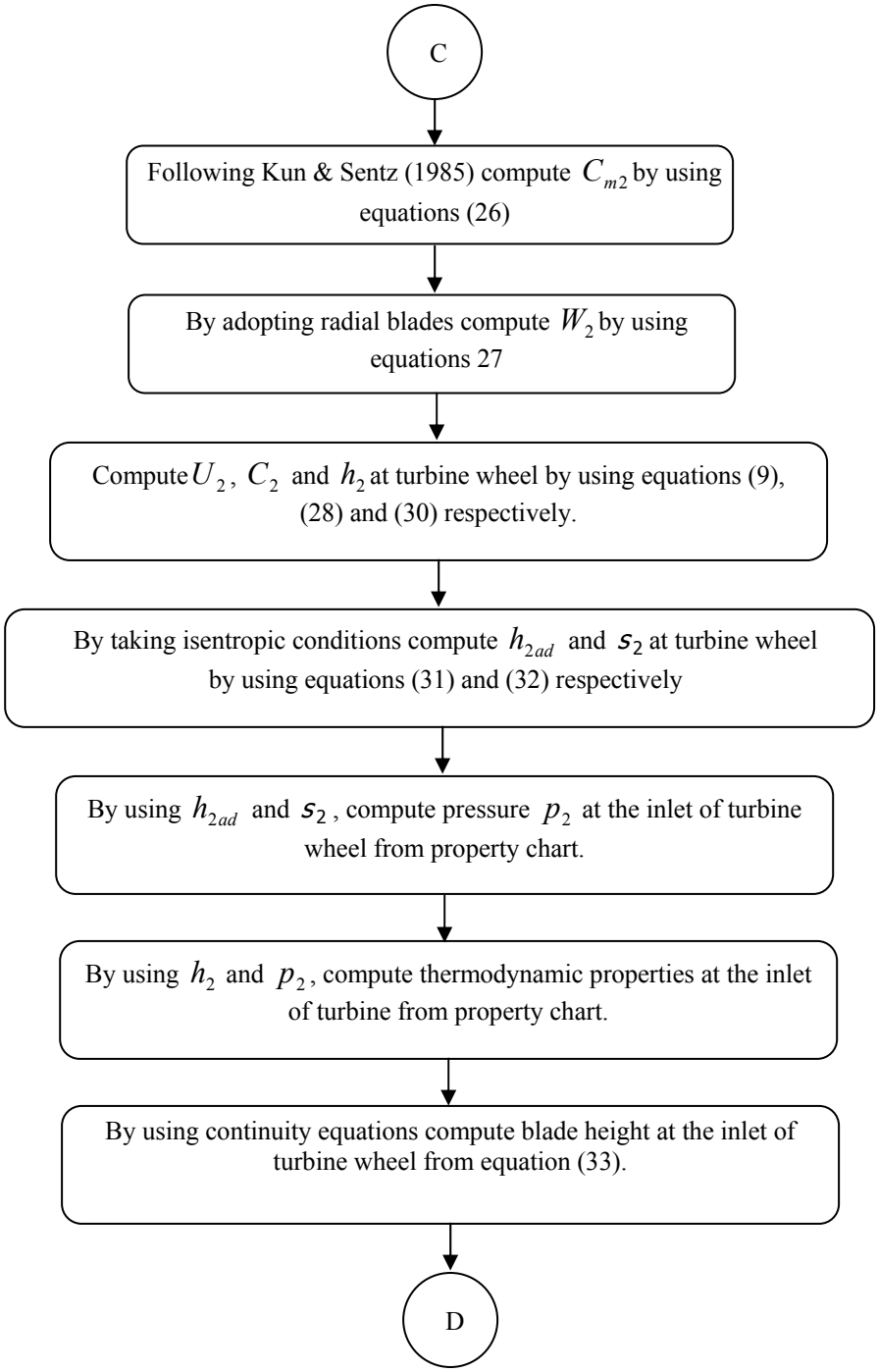
C
Following Kun & Sentz (1985) compute C_{m2} by using equations (26)
By adopting radial blades compute W_2 by using equations 27
Compute U_2, C_2 and h_2 at turbine wheel by using equations (9), (28) and (30) respectively.
By taking isentropic conditions compute h_{2ad} and s_2 at turbine wheel by using equations (31) and (32) respectively
By using h_{2ad} and s_2, compute pressure p_2 at the inlet of turbine wheel from property chart.
By using h_2 and p_2, compute thermodynamic properties at the inlet of turbine from property chart.
By using continuity equations compute blade height at the inlet of turbine wheel from equation (33).
D

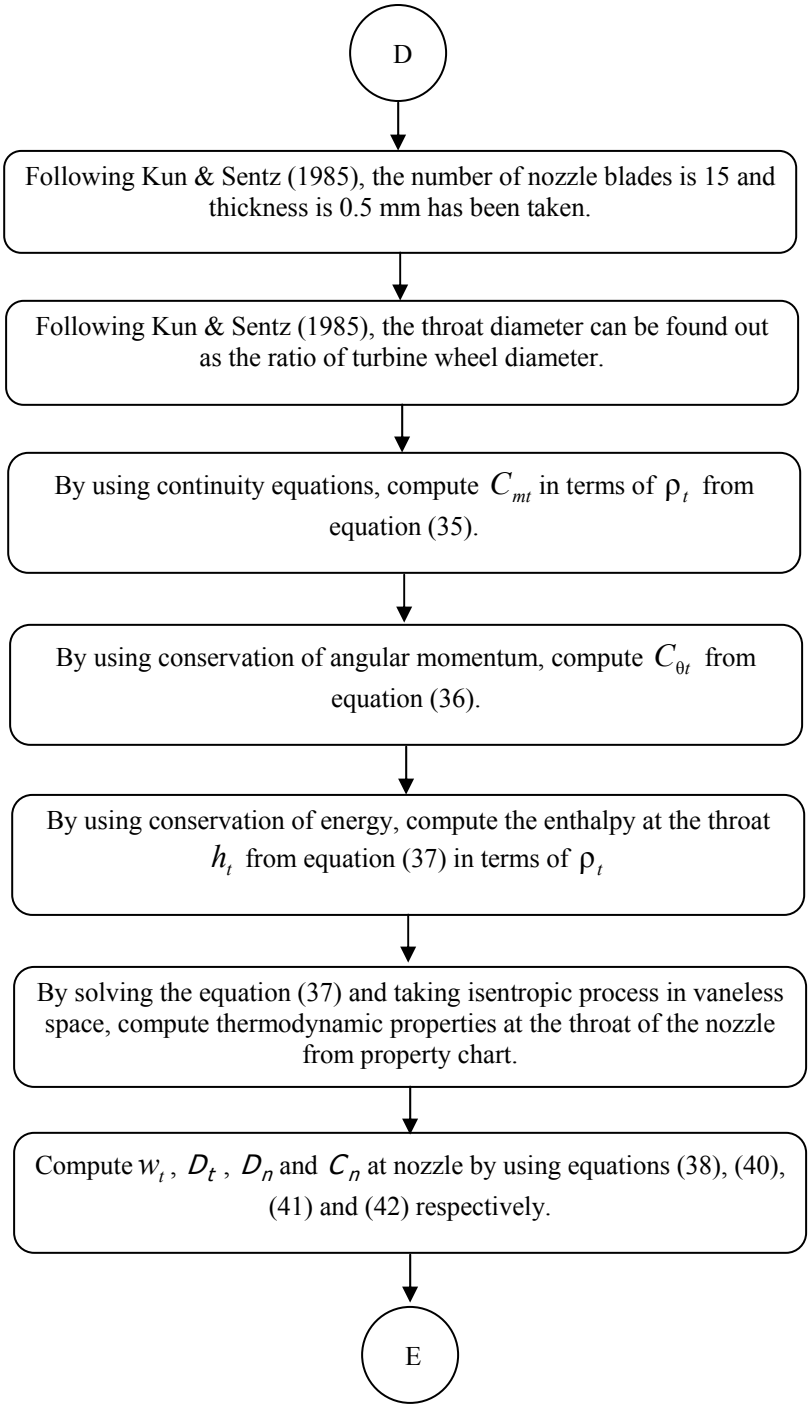

Figure 9: Flow chart for calculation of state properties and dimension of cryogenic turboexpander

References

Abidat M., Hamidou M.K., Hachemi M. and Hamel M., 2006. Design and flow analysis of radial and mixed flow turbine volutes, *European Conference on Computational Fluid Dynamics*, ECCOMAS CFD Egmond Aan Zee, The Netherlands.

Baines, N. 2002. Radial and mixed flow turbine options for high boost turbochargers, *7th international conference on Turbochargers and Turbocharging*, London, pp. 35-44.

Balje, O. E. 1981. Turbomachines, John Wiley and Sons, London.

Balje, O. E. 1970. Loss and flow path studies on centrifugal compressors, *Part-II Trans ASME J Eng Power*, No-70, pp. 275-299.

Beasley, S. A. and Halford, P. 1965. Development of a high purity nitrogen plant using expansion turbine with gas bearing, *Advances in Cryogenic Engineering*, V10B, pp. 27-39.

Bruce, G. J. 1998. Computer-aided turbomachinery design system, *I Mech E Conference on Turbochargers*, I Mech E Publications, London, C554/026/98, pp. 3-22.

Denton, J. D. 1996. The turboexpander - a design, make and test student project ASME-96-GT- 191.

Descombes G., Maroteaux F., Moreno N., Jullien J. 2003. Analysis of energy conversion within a radial turbine stage, *Int. J. Thermodynamics*, Vol.6, No.1, pp.41-48.

Dixon, S. L. 1978. *Fluid Mechanics and Thermodynamics of Turbomachinery* (3rd ed) Pergamon Press, London.

Ghosh, S. K., Seshaiah, N., Sahoo. R. K., Sarangi. S. K. 2005. Design of turboexpander for cryogenic applications, *Indian J. Cryogenics*, Special Issue Vol-2, pp. 75-81.

Ghosh, S. K., Sahoo. R. K., Sarangi. S. K. 2009. A computational approach to the design of a cryogenic turbine blade profile, *International Journal of Engineering, Science and Technology*, Vol. 1, No. 1, pp. 43-60.

Ghosh, P. 2002. Analytical and Experimental Studies on Cryogenic Turboexpanders Ph.D dissertation, IIT Kharagpur

Hasselgruber, H. 1958, Stromungsgerechte gestaltung der laufrader von radialkompressoren mit axialem laufradeintrict *Konstruction*, Vol. 10, No. 1, pp. 22 (in German)

Ino, N., Machida, A. and Ttsugawa, K. 1992. Development of high expansion ratio He turboexpander, *Advances in Cryogenic Engineering*, V37B, pp. 835-844.

Jekat, W. K. 1957. An impulse type expansion turbine, *Advances in Cryogenic Engineering*, V2, 250-260.

Jadeja, H. T., Mitter, A. and Chakrabarty, H. D. 1985. Turboexpander application for cryoprocessing of nitrogen and related gases Proceedings of inconcryo, 85 Indian Cryogenic Council, Tata McGraw, pp. 85-101.

Kun, L .C. and Sentz, R. N. 1985. High efficiency expansion turbines in air separation and liquefaction plants, *International Conference on Production and Purification of Coal Gas & Separation of Air*, Beijing, China, pp. 1-21

Kun, L. C. 1987. Expansion turbines and refrigeration for gas separation and liquefaction, *Advances in Cryogenic Engineering*, V33, pp. 963-973.

Lemmon, E. W., Jacobsen, R. T., Penoncello, S. G. and Beyerlein, S. W., 1995. ALLPROPS 4.2 – Computer programs for calculating thermodynamic properties of fluids of engineering interest, Centre for Applied Thermodynamic Studies, University of Idaho

Rohlik, Harold E. 1968. Analytical determination of radial inflow turbine geometry for maximum efficiency NASA TN D-4384.

Sixsmith, H. 1971. Miniature expansion turbines, C A Bailey (Ed), Advanced Cryogenics Plenum Press, London pp. 225-243.

Sixsmith, H., Valenjuela, J. and Swift, W. L. 1988, Small Turbo-Brayton cryocoolers *Advances in Cryogenic Engineering* , V34, 827-836

Stewart, W.L. and Glassman, A. J. 1973. Turbine Design and Application, NASA SP-290, London, Vol. 2, pp. 1-25.

Von Der Nuell , W. T. 1952. Single-stage radial turbine for gaseous substances with high rotative and low specific speed, *Trans ASME*, V74, pp. 499-515.

Whitfield, A. and Baines, N. C. 1990. *Design of Radial Turbomachines*, Longman Scientific & Technical, NewYork.

Yang, K. J., He, H. B., Ke, G. and Li, G. Y. 1990. Application and test of miniature gas bearing turbines, *Advances in Cryogenic Engineering*, V35, pp. 997-1003.

Biographical notes

Dr. Subrata Kumar Ghosh is Senior Lecturer in the Department of Mechanical Engineering & Mining Machinery Engineering at ISM, Dhanbad, India. Before joining at ISM He was Lecturer at BIT, Mesra. His research has focused on Thermal Engineering. He is the author and coauthor of over 8 articles, which have appeared in journals such as *Applied Thermal Engineering, Indian Journal of Cryogenics*, and several seminars.

Received December 2009
Accepted January 2010
Final acceptance in revised form March 2010